



# A comparison of hydro-geochemistry and stable isotope composition of travertine-depositing springs, Garab in NE Iran and Pamukkale in SW Turkey

Hossein Mohammadzadeh<sup>1,2</sup> · Mohammad Reza Mansouri Daneshvar<sup>3</sup>

Accepted: 12 February 2020

© Springer-Verlag GmbH Germany, part of Springer Nature 2020

## Abstract

In this study, the hydro-geochemistry and stable isotope compositions ( $\delta^{18}\text{O}$ ,  $\delta^2\text{H}$ , and  $\delta^{13}\text{C}$ ) of travertine-depositing springs were investigated in two regions of Garab and Pamukkale, located in NE-Iran and SW-Turkey, respectively. The physical, chemical and isotopic dataset of water and travertine samples were obtained in situ measurements, laboratory analysis and from the literature. According to the high EC values ( $\sim 2400$  and  $\sim 10,500$   $\mu\text{S}/\text{cm}$ ), the average  $\delta^{13}\text{C}_{\text{DIC}}$  values of water samples (10.4 and 7.2‰ VPDB), and its  $\delta^{13}\text{C}-\text{CO}_2$  values (1.5 and  $-1.8$ ‰ VPDB), it seems that the Garab and Pamukkale spring water were supplying from deep thermal groundwater with thermogenic origins and with contribution of carbonate dissolution through the rock-water interactions process. The more concentrations of  $\text{Na}^+$ ,  $\text{K}^+$ , and  $\text{Cl}^-$  in Garab water are related to subsequent admixture processes, which is originated from dissolving overloaded impure dissolve materials during upwelling water toward the ground level. The more enriched  $\delta^{13}\text{C}$  and  $\delta^{18}\text{O}$  values of Garab travertine samples (10.4 and  $-7.1$ ‰ VPDB, respectively) than that of Pamukkale travertine (7.2 and  $-10.4$ ‰ VPDB, respectively) is due to more  $\text{CO}_2$  degassing. The isotopic compositions of precipitation in both Garab ( $\delta^2\text{H} = 7.2 * \delta^{18}\text{O} + 11.2$ ‰) and Pamukkale ( $\delta^2\text{H} = 8 * \delta^{18}\text{O} + 16$ ‰) areas are characterized by greater d-excess compared to GMWL but smaller than of Mediterranean area. Although the isotopic compositions of both Garab and Pamukkale springs show the meteoric origin; however, the deviation from meteoric water lines is probably evident to oxygen isotope exchange with the deep host bedrock.

**Keywords** Hydro-geochemistry · Stable isotopes · Travertine-depositing springs · Garab · Pamukkale

## Introduction

Travertine deposition is the result of  $\text{CaCO}_3$  precipitation from hydrothermal springs rising along with fractures and faults in Earth's crust (Pentecost 2005; Crossey et al. 2006; Pedley 2009). The geological and hydrogeochemical

analysis of travertine regions have been widely studied in the world such as in Turkey (Altunel and Hancock 1993; Atabey 2002; Uysal et al. 2007; Bayari et al. 2009; Kele et al. 2011; Özkul et al. 2013), Italy (Minissale et al. 2002; Anzalone et al. 2007; Brogi and Capezzuoli 2009; Brogi et al. 2010; Petitta et al. 2011), USA (Chafetz and Guidry 2003; Hershey et al. 2010) and Iran (Mohammadzadeh 2009; Mansouri Daneshvar 2015; Mansouri Daneshvar and Pourali 2015; Mohammadzadeh and Kazemi 2017; Goleij et al. 2018).

The geomorphological landform of carbonate deposition in the Garab region in NE Iran has been patched structurally into both robust thermogenic travertine and fragile meteoric tufa (Mansouri Daneshvar 2015). Due to active lithogenesis and groundwater discharge from several springs, this region has sufficient interest in hydrological and geological studies in Iran. Mansouri Daneshvar and Pourali (2015) have claimed that the geomorphological processes and products of the Garab region in Iran are similar to travertine depositions of the Denizli basin in SW Turkey.

✉ Hossein Mohammadzadeh  
mohammadzadeh@um.ac.ir

Mohammad Reza Mansouri Daneshvar  
mrm\_daneshvar2012@yahoo.com

<sup>1</sup> Department of Geology, Faculty of Science, Ferdowsi University of Mashhad, P.O. Box: 91775-1436, Mashhad, Iran

<sup>2</sup> Groundwater and Geothermal Research Center (GRC), Water and Environment Research Institute, Ferdowsi University of Mashhad, Mashhad, Iran

<sup>3</sup> Department of Geography and Natural Hazards, Research Institute of Shakhes Pajouh, Isfahan, Iran

Several studies have focused on the hydrogeology, geo-thermal potential, and chemistry of thermal waters in the Denizli basin and its main region named as Pamukkale (e.g., Ekmekçi et al. 1995; Şimşek et al. 2000). Filiz (1984), who first published stable isotopic data of Pamukkale springs, concluded that the CO<sub>2</sub> content of the spring water came from magmatic resources. Altunel and Hancock (1993) classified the Pamukkale travertine according to its morphology, while Altunel (1994) and Hancock and Altunel (1997) investigated the relationship between active fissuring, faulting, and travertine deposition. Çakır (1999) described structural attributes of the Pamukkale travertine paying particular attention to the fault zone. Özkul et al. (2002) described differently litho-facies types from travertine in the Denizli Basin. In recent years, various studies have focused on new geochemical investigations and systematic stable isotope and trace element analysis in the Pamukkale region (e.g., Zedef et al. 2000; Şimşek 2003; Uysal et al. 2007; Kele et al. 2011; Özkul et al. 2013).

Now, the present paper aims to investigate the hydro-geochemistry and stable isotope compositions of travertine-depositing springs in both Garab and Pamukkale regions in NE Iran and SW Turkey, respectively. Accordingly, the results are compared together. The main novelty and significance of this research is the comparison of two travertine springs, which are located along the Alp-Himalayan volcanic belt and may indicate a possible similar mechanism of hydro-geology. Hence, the results of this research would improve the basic knowledge of travertine depositing in the Middle East and Mediterranean regions. Besides, it is for the first time that the stable isotope composition of the travertine depositing spring of Garab in NE-Iran was presented.

## Geographical and geological setting

In the present study, two regions are accounted for considering study areas named as Garab region in Iran and Pamukkale region in Turkey (Fig. 1a). Garab region with a total surface area of 5.8 Km<sup>2</sup>, is located geographically in the southeastern parts of Binaloud mountainous zone, NE Iran between latitude 35° 58'–36° 00' N and longitude 59° 37'–59° 40' E (Fig. 1b). In this region, precipitated travertine rocks have emerged geologically among the Neogene red conglomerates and Quaternary sediments (Mansouri Daneshvar 2015). This region with a mean topographic elevation of 1300 m a.s.l. (Fig. 2a), which consists of the main volcano-shaped spring and a terraced hill with active drainage, has a semi-arid climate with mean annual precipitation and temperature of 235 mm and 14.5 °C, respectively. The Garab travertine is theoretically a metamorphic horst zone affected by tectonic of Binaloud extensional faults. The Binaloud tectonic includes meta-ophiolites,

meta-sedimentary rocks, and meta-flysch sequences interpreted as remnants of the Paleo-Tethys fossil ocean (Karim-pour et al. 2010).

Pamukkale region as a UNESCO-sponsored world cultural heritage sites is located geographically in the northern parts of Denizli Basin, SW Turkey between latitude 37° 54'–37° 57' N and longitude 29° 05'–29° 10' E (Fig. 1c). This region with a mean topographic elevation of 300 meters a.s.l. (Fig. 2b), which consists of mainly four springs and numerous seeps that emerged from the metamorphic bedrock and terraced travertine zone, has a temperate Mediterranean climate with mean annual precipitation and temperature of 550 mm and 13.5 °C, respectively (Özkul et al. 2010). Denizli Basin, which belongs to the extensive Buyuk Menderes graben system (Şimşek 2003), is home for numerous active (e.g., Pamukkale, Karahayit) and inactive (e.g., Akköy, Karakaya) thermal travertine-depositing springs with a total surface area of 100 Km<sup>2</sup> (Özkul et al. 2002). Denizli Neogene depression has been controlled by Babadağ fault to the south and then, by the early Quaternary, Denizli basin was developed into a graben due to activity associated with the Pamukkale fault to the north, which led to the formation of significant travertine precipitation in the basin (Alçiçek et al. 2007).

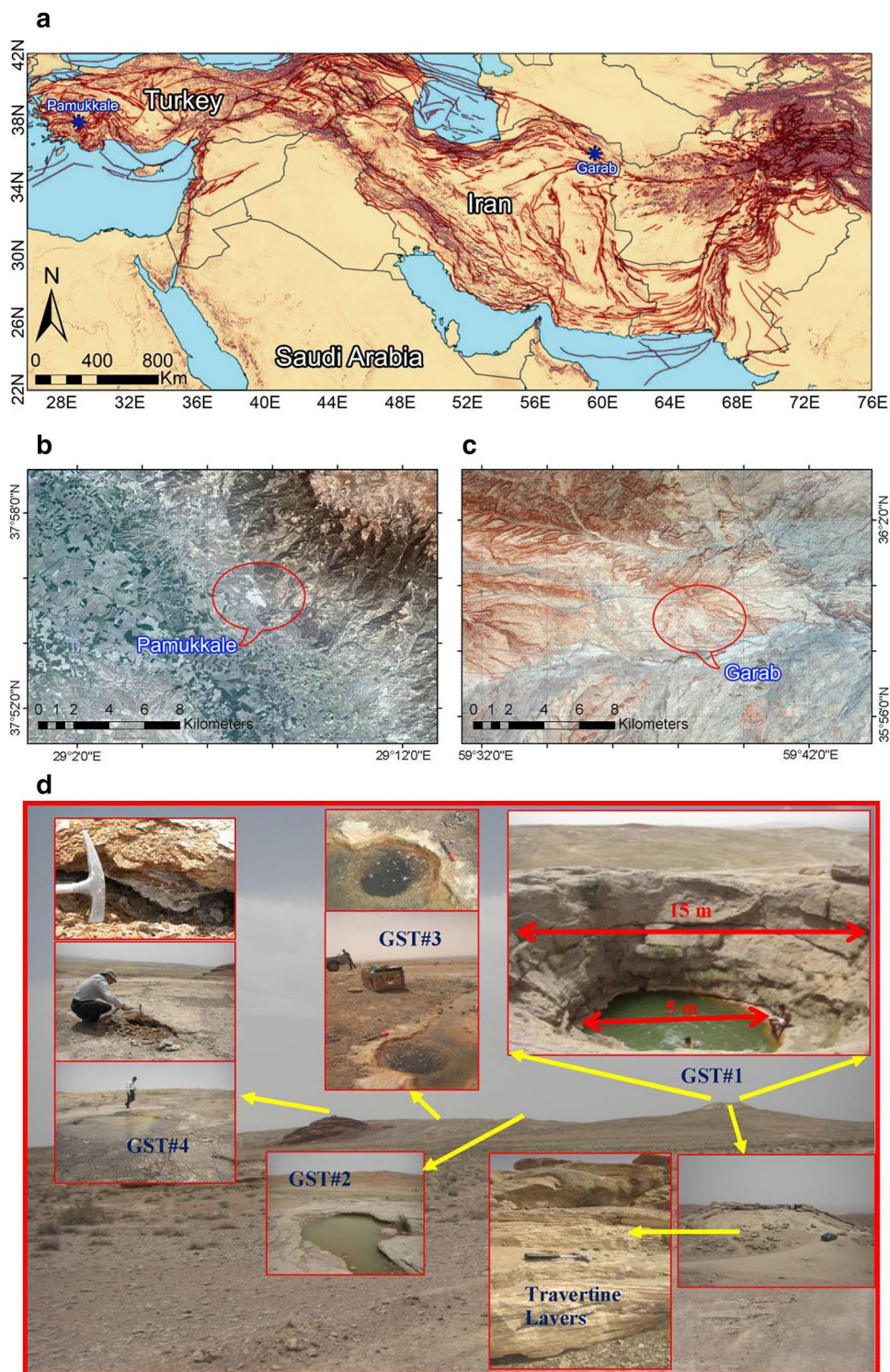
## Materials and methods

### Field sampling, analytical methods and data collection

To hydro-geochemistry analyses of the Garab region, the water and rock samples were collected during fieldwork (Fig. 1d). The physical and chemical datasets of water samples were obtained from in situ measurements and laboratory analysis. Field geochemical parameters, including T, pH, EC, and TDS, were measured during sampling using appropriate meters. Water samples for major anions and cations and δ<sup>2</sup>H and δ<sup>18</sup>O of water were collected in high-density polyethylene (HDPE) 25 ml plastic bottles. All samples were filtered using 0.45 µm membranes, and the cation samples were acidified using concentrated HNO<sub>3</sub> acid. Some 40 mL filtered samples were collected using amber glass bottles to measure concentrations and δ<sup>13</sup>C of DIC. For methane and CO<sub>2</sub> (concentration and isotopes) measurements, unfiltered water samples were collected in 125 mL Wheaton glass bottles with headspace. Mohammadzadeh and Clark (2011) have explained detailed procedures of water sampling for isotope analysis.

The concentrations of main cations (Ca<sup>2+</sup>, Mg<sup>2+</sup>, Na<sup>+</sup> and K<sup>+</sup>) were measured using Inductively Coupled Plasma Atomic Emission Spectroscopy (ICP-AES). The Ion chromatography (IC) was used to measure the inorganic anions

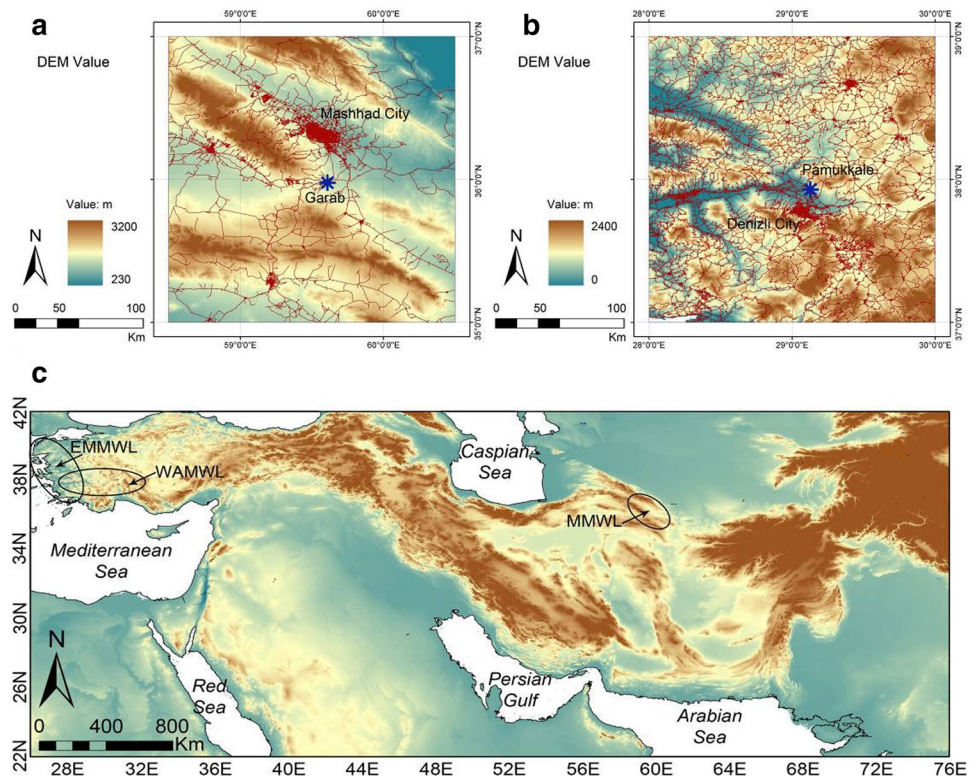
**Fig. 1** General visualizations of the study areas **a** Geographical position of the study areas, **b** Garab region in NE Iran, **c** Pamukkale region in SW Turkey, and **d** sampling locations in Garab area



( $\text{Cl}^-$ ,  $\text{SO}_4^{2-}$  and  $\text{NO}_3^-$ ) concentrations of the samples and the bicarbonate ( $\text{HCO}_3^-$ ) concentrations were determined by titration. The  $\delta^{18}\text{O}$  and  $\delta^2\text{H}$  of the water samples were measured using a Gasbench and DeltaPlus XP continuous-flow isotope-ratio mass spectrometer (CF-IRMS, with analytical precision of  $\pm 0.15$  and  $\pm 2.0\%$ , respectively). The

concentration and  $^{13}\text{C}$ -isotopic compositions of DIC were measured using a Total Carbon Analyzer (TCA-OI Instruments Model 1010) interfaced with CF-IRMS, with analytical precision of  $\pm 0.1\%$  and  $\pm 0.15\%$  for concentration and  $^{13}\text{C}$ , respectively (Mohammadzadeh et al. 2005). Headspace samples were analyzed for methane concentration,  $\delta^{13}\text{C}_{\text{CH}_4}$ ,

**Fig. 2** Topographic maps of the study areas **a** Garab region, **b** Pamukkale region, and **c** the areas of Mashhad meteoric water line (MMWL), West Anatolian meteoric water line (WAMWL), and Eastern Mediterranean meteoric water line (EMMWL)



and  $\delta^{13}\text{C}_{\text{CO}_2}$  using gas chromatography (GC) combustion system (GCC III) interfaced with a CF-IRMS with analytical precision of  $\pm 0.2$  to  $\pm 0.3\%$ . All geochemical analyses of ions and the isotopic analyses of water, rock, and gases samples were performed at the Geochemistry and G. G. Hatch Stable Isotope laboratories at the University of Ottawa. The geochemical components of travertine rock samples (consisted  $\text{SiO}_2$ ,  $\text{TiO}_2$ ,  $\text{Al}_2\text{O}_3$ ,  $\text{Fe}_2\text{O}_3$ ,  $\text{MgO}$ ,  $\text{CaO}$ ,  $\text{Na}_2\text{O}$ , and  $\text{K}_2\text{O}$ ) were prepared based on Mansouri Daneshvar and Pourali (2015) and Kele et al. (2011) for the Garab and Pamukkale study areas.

Analytical and logical procedures of hydro-geochemical sampling of isotope analysis have been explained in previous studies (e.g., Han and Liu 2004; Ryu et al. 2007; Han et al. 2010; Ma et al. 2011; Keshavarzi et al. 2011; Pazand et al. 2012; Zhang et al. 2004; Lang et al. 2006; Di Benedetto et al. 2011; Kele et al. 2011; Özkul et al. 2013). The mean values of hydro-geochemistry and stable isotope data were considered based on Kele et al. (2011) for the Pamukkale region in Turkey to compare the results.

### Data visualization

Several types of plots (composition diagrams) were implemented based on the global literature and using Minipet\_2.02 and GW\_Chart software to visualize the hydrological, geochemical, and isotope data. The Piper trilateral diagram (Piper 1944) was used to identify chemical properties.

Ternary diagrams of  $\text{CaO-MgO-SiO}_2$ ,  $\text{MgO-Al}_2\text{O}_3\text{-SiO}_2$ , and  $\text{CaO-MgO-other}$  compositions were used (Von Eynatten et al. 2002) to visualize compositional data. Geochemical plots of  $(\text{Na} + \text{K})/\text{HCO}_3$  against  $(\text{Mg} + \text{Ca})/\text{HCO}_3$  and  $\text{Mg}/\text{Ca}$  against  $\text{Na}/\text{Ca}$  were produced after Han and Liu (2004). Also, the geochemical plot of TDS against  $\text{Na}/(\text{Na} + \text{Ca})$  was produced after Ryu et al. (2007). To visualize the stable isotope compositions plot of  $\delta$  oxygen-18 ( $\delta^{18}\text{O}$ ) against  $\delta$  deuterium ( $\delta^2\text{H}$  or  $\delta^2\text{H}$ ) were implemented after Craig (1961).

### Results

The results of filed parameters measurements and hydro-geochemical results of Garab and Pamukkale water samples were arranged in Table 1 and the chemical results of rock samples analysis, presented in Table 2. The results of the stable isotope composition of spring water,  $\text{CO}_2$  gas, and travertine for both Garab and Pamukkale areas were presented in Table 3.

### Hydro-geochemistry and geochemical properties of Garab and Pamukkale

The EC value of thermogenic water normally varies in the 1000–10,000  $\mu\text{S}/\text{cm}$  range (Pentecost 2005). Therefore, the Garab and Pamukkale spring water (with EC values of  $\sim 10,500$  and  $\sim 2400$   $\mu\text{S}/\text{cm}$ , respectively) are of thermogenic

**Table 1** Concentrations of field and chemical components of water samples in Garab study area (all data in mg/l if nothing else mentioned)

| Sample ID                                | Elevation (m.a.s.l.) | Field Parameters |     |            |      |      | Anions (ppm)    |                               |                               |                              |                  | Cations (ppm)    |     |                  |                 |                |                  |                 |
|--|----------------------|------------------|-----|------------|------|------|-----------------|-------------------------------|-------------------------------|------------------------------|------------------|------------------|-----|------------------|-----------------|----------------|------------------|-----------------|
|  |                      | T (°C)           | PH  | EC (µS/cm) | TDS  | TH*  | Cl <sup>-</sup> | HCO <sub>3</sub> <sup>-</sup> | SO <sub>4</sub> <sup>2-</sup> | NO <sub>3</sub> <sup>-</sup> | Ba <sup>2+</sup> | Ca <sup>2+</sup> | Fe  | Mg <sup>2+</sup> | Na <sup>+</sup> | K <sup>+</sup> | Si <sup>2+</sup> | Sr <sup>+</sup> |
| <b>Garab</b>                             |                      |                  |     |            |      |      |                 |                               |                               |                              |                  |                  |     |                  |                 |                |                  |                 |
| GST#1                                    | 1333                 | 21.3             | 6.5 | 9670       | 5300 | 1177 | 2690            | 1090                          | 1.2                           | 46.7                         | 277              | 90.2             | 118 | 3155             | 119             | 385            | 10.7             |                 |
| GST#1                                    | 1333                 | 24.0             | 6.7 | 11,000     | 6930 | 1444 | 2528            | 994                           |                               | 410                          | 410              |                  | 102 | 2065             | 125             |                |                  |                 |
| GST#2                                    | 1342                 | 27.7             | 6.2 | 10,280     | 5660 | 1478 | 3036            | 1474                          |                               | 399                          | 399              |                  | 117 | 3078             | 108             | 116            | 13.3             |                 |
| GST#3                                    | 1339                 | 21.8             | 6.7 | 10,670     | 5870 | 1555 | 2846            | 1476                          |                               | 415                          | 415              |                  | 126 | 2969             | 118             | 91             | 13.0             |                 |
| GST#4                                    | 1346                 | 26.6             | 6.1 | 10,520     | 5810 | 1673 | 2903            | 1461                          |                               | 490                          | 490              |                  | 109 | 3386             | 180             | 456            | 14.5             |                 |
| Average                                  | 1339                 | 24.3             | 6.4 | 10,428     | 5914 | 1464 | 2801            | 1299                          | 1.2                           | 47.8                         | 398              | 90.2             | 114 | 2931             | 130             | 262            | 12.9             |                 |
| <b>Pamukkale (from Kele et al. 2011)</b> |                      |                  |     |            |      |      |                 |                               |                               |                              |                  |                  |     |                  |                 |                |                  |                 |
| Min                                      | 290                  | 32.9             | 6.0 | 2300       | 1179 | 1468 | 10              | 660                           | 1.3                           | 0.02                         | 446              | 1.4              | 86  | 39               | 5               | 20.5           | 6.1              |                 |
| Max                                      | 366                  | 56.1             | 6.9 | 3000       | 1188 | 1823 | 27              | 1096                          | 2.1                           | 0.06                         | 537              | 2.9              | 117 | 128              | 26              | 28.7           | 10.7             |                 |
| Average                                  | 335                  | 36.7             | 6.2 | 2400       | 1186 | 1679 | 19              | 918                           | 1.7                           | 0.05                         | 499              | 2.3              | 105 | 89               | 17              | 24.0           | 8.7              |                 |

\*TH = 2.5 Ca<sup>2+</sup> + 4.11 Mg<sup>2+</sup>

**Table 2** Average concentrations of geochemical components of rock (travertine) samples in both Garab and Pamukkale areas

| Components                     | Garab (%)* | Pamukkale (%)** |
|--------------------------------|------------|-----------------|
| TiO <sub>2</sub>               | 1.02       | 0.00            |
| Al <sub>2</sub> O <sub>3</sub> | 0.15       | 0.25            |
| Fe <sub>2</sub> O <sub>3</sub> | 8.78       | 0.07            |
| MgO                            | 7.17       | 0.61            |
| CaO                            | 59.24      | 54.94           |
| Na <sub>2</sub> O              | 5.98       | 0.13            |
| K <sub>2</sub> O               | 5.23       | 0.07            |
| SiO <sub>2</sub>               | -          | 1.73            |
| LOI (Loss on Ignition)         | 10.23      | 42.00           |
| Total                          | 99.98      | 99.80           |

\* Mansouri Daneshvar and Pourali (2015)

\*\*Kele et al. (2011)

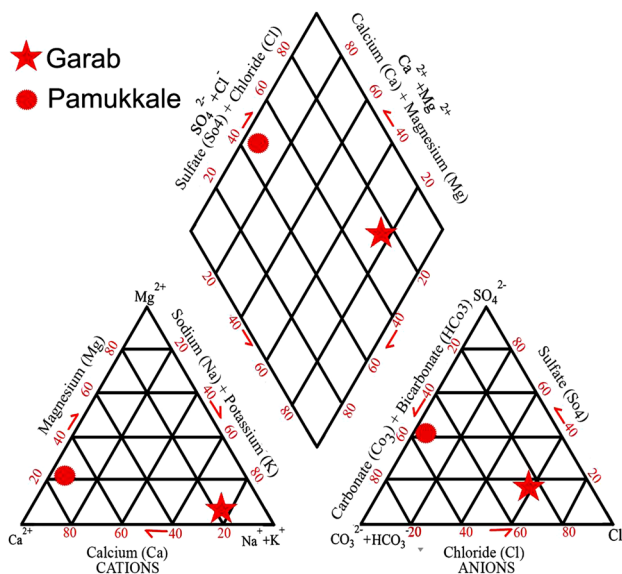
origin. According to the data listed in Table 1, the average concentrations of Na<sup>+</sup> and Cl<sup>-</sup> with values of 2931 and 2801 mg/l, respectively, represent the dominant cations and anions in the Garab area. These high concentrations of Na<sup>+</sup> and Cl<sup>-</sup> may relate to the saline soils (Na-Cl) or evaporative strata in paths of upwelling water. Total average concentrations of Ca<sup>2+</sup> and Mg<sup>2+</sup> were calculated about 512 mg/l, relating to calcium carbonate and dolomite (about 12%). According to the position plotted in the Piper trilateral diagram, the chemical property of the Garab karstic aquifer was identified as Na-Cl and Ca-HCO<sub>3</sub>-SO<sub>4</sub> (Fig. 3). The cations and anions concentrations display the decreasing order of Na<sup>+</sup> > Ca<sup>2+</sup> > Si<sup>2+</sup> > K<sup>+</sup> > Mg<sup>2+</sup> and Cl<sup>-</sup> > HCO<sub>3</sub><sup>-</sup> > SO<sub>4</sub><sup>2-</sup> > NO<sub>3</sub><sup>-</sup>, respectively. The high concentration of HCO<sub>3</sub><sup>-</sup> and SO<sub>4</sub><sup>2-</sup> as predominant anions in the water attributes mainly to calcium carbonate (CaCO<sub>3</sub>) and gypsum (CaSO<sub>4</sub>·2H<sub>2</sub>O) lithology. The calcium, bicarbonate, and sulfate concentrations show that these ions originate from the dissolution of limestone and evaporate units (Dominguez-Villar et al. 2017). The high concentration of Na is also can be related to salty units that can be more concentrated by evaporation in warm and dry seasons in this area (Mansouri Daneshvar 2015; Goleij et al. 2018). The hydro-geochemical analyses of spring water in Pamukkale region shows that Ca<sup>2+</sup> and Mg<sup>2+</sup> (with average values of 499 and 105 mg/l, respectively) and HCO<sub>3</sub><sup>-</sup> and SO<sub>4</sub><sup>2-</sup> (with average values of 1046 and 918 mg/l, respectively), are the major cations and anions and the main water type is calcium bicarbonate that relates to a karst aquifer (Table 1). Total ion concentrations of Ca<sup>2+</sup> and Mg<sup>2+</sup> were about 604 mg/l, resulting in calcium carbonate and dolomite (about 48%). The chemical property of the Pamukkale aquifer was identified as Ca-HCO<sub>3</sub> and Mg-SO<sub>4</sub> (Fig. 3) and the cations and anions display the decreasing order of Ca<sup>2+</sup> > Mg<sup>2+</sup> > Na<sup>+</sup> > Si<sup>2+</sup> > K<sup>+</sup> and

**Table 3** Stable isotope compositions of water, gas and rock (travertine) samples in the study areas (all water isotope in ‰VSMOW and other isotopes in ‰VPDB)

| Sample ID                         | H <sub>2</sub> O |                   | DIC |                   | CO <sub>2</sub> * |                   | Travertine**      |                   |
|-----------------------------------|------------------|-------------------|-----|-------------------|-------------------|-------------------|-------------------|-------------------|
|                                   | δ <sup>2</sup> H | δ <sup>18</sup> O | Ppm | δ <sup>13</sup> C | mg/l              | δ <sup>13</sup> C | δ <sup>13</sup> C | δ <sup>18</sup> O |
| Garab                             |                  |                   |     |                   |                   |                   |                   |                   |
| GST#1                             | -70.8            | -9.7              | 280 | 4.9               | 316               | 2.4 (1.5)         | 10.0 (9.1)        | -6.8 (-7.3)       |
| GST#2                             | -71.3            | -9.8              | 300 | 6.1               |                   | 2.0               |                   |                   |
| GST#3                             | -59.8            | -7.6              | 330 | 5.7               |                   | -1.5 (1.5)        | 10.0 (10.3)       | -7.2 (-7.1)       |
| GST#4                             | -70.1            | -10.0             | 370 | 6.6               |                   | 0.6 (3.8)         | 11.9 (11.3)       | -7.0 (-7.4)       |
| Average                           | -68.0            | -9.3              | 320 | 5.8               | 316               | 0.9 (1.5)         | 10.4              | -7.1              |
| Pamukkale (from Kele et al. 2011) |                  |                   |     |                   |                   |                   |                   |                   |
| Min                               | -60.0            | -9.0              |     |                   | 400               | (-4.4)            | 5.1               | -12.8             |
| Max                               | -58.5            | -7.6              |     |                   | 1200              | (3.5)             | 11.7              | -8.9              |
| Average                           | -58.7            | -8.7              |     | -1.0              | 673               | (-1.8)            | 7.2               | -10.5             |

\*Values within the parentheses are calculated using  $\delta^{13}\text{C}_{\text{CO}_2} = 1.2 \delta^{13}\text{C}_{\text{travertine}} - 10.5$  (Panichi and Tongiorgi 1976)

\*\*Values within the parentheses are duplicate measurements

**Fig. 3** Piper diagram of hydro-geochemical properties of water samples in Garab and Pamukkale regions

$\text{HCO}_3^- > \text{SO}_4^{2-} > \text{Cl}^- > \text{CO}_3^{2-}$ , which is different from of Garab.

Different compositions diagrams of geochemical plots of Mg/Ca against Na/Ca, TDS against Na/(Na + Ca), and (Na + K)/HCO<sub>3</sub> against (Mg + Ca)/HCO<sub>3</sub> were produced for water samples in both Garab and Pamukkale regions (Fig. 4). This figure revealed that Garab hydrochemistry is near to evaporative seawaters affecting with silicate weathering. Hence, hydro-geochemistry of spring water in the Garab region may become originated from carbonate lithology, but has been controlled by evaporating admixtures and silicate weathering during upwelling from underground to the ground level. Pamukkale hydrochemistry is

close to limestone without any weathering effect, exposing its origin depending on carbonate bedrock in a karst aquifer.

Based on the chemical results of rock samples analysis, presented in Table 2, the composition of the rock samples in both Garab and Pamukkale regions was demonstrated as CaO with values 59.24% and 56.14%, respectively. In this regard, the main calcite mineralogy of carbonate rocks was detected based on the plot of CaO–MgO–SiO<sub>2</sub>, MgO–Al<sub>2</sub>O<sub>3</sub>–SiO<sub>2</sub>, and CaO–MgO–other compositions ternary diagrams (Fig. 5). Concomitantly, Goleij et al. (2018) revealed that travertine rocks in the Garab area are composed of calcite and aragonite minerals.

### Water and travertine stable isotopes (δ<sup>18</sup>O, δ<sup>2</sup>H, δ<sup>13</sup>C) compositions of Garab and Pamukkale

In the Garab region, the δ<sup>18</sup>O and δ<sup>2</sup>H values of the spring water were measured about -9.3 and -68.0‰ VSMOW, respectively, and the δ<sup>13</sup>C and δ<sup>18</sup>O values of rock samples (travertine) were measured about 10.4 and -7.1‰ VPDB, respectively. In this region, the δ<sup>13</sup>C-DIC and δ<sup>13</sup>C- of free CO<sub>2</sub> gas were measured as 5.8 and 0.9‰ VPDB, respectively. The Garab spring water samples have almost similar stable isotope compositions values of water to those measured at Pamukkale spring water (-8.7, -58.7‰ VSMOW for δ<sup>18</sup>O and δ<sup>2</sup>H, respectively). However, the δ<sup>13</sup>C-DIC values of Pamukkale spring water samples are much depleted (-1.0‰ VPDB). The δ<sup>13</sup>C and δ<sup>18</sup>O values of travertine samples were measured about 7.2 and -10.4‰ VPDB, respectively, which are depleted about 3.5‰ VPDB than that of average values of Garab springs (Table 3).

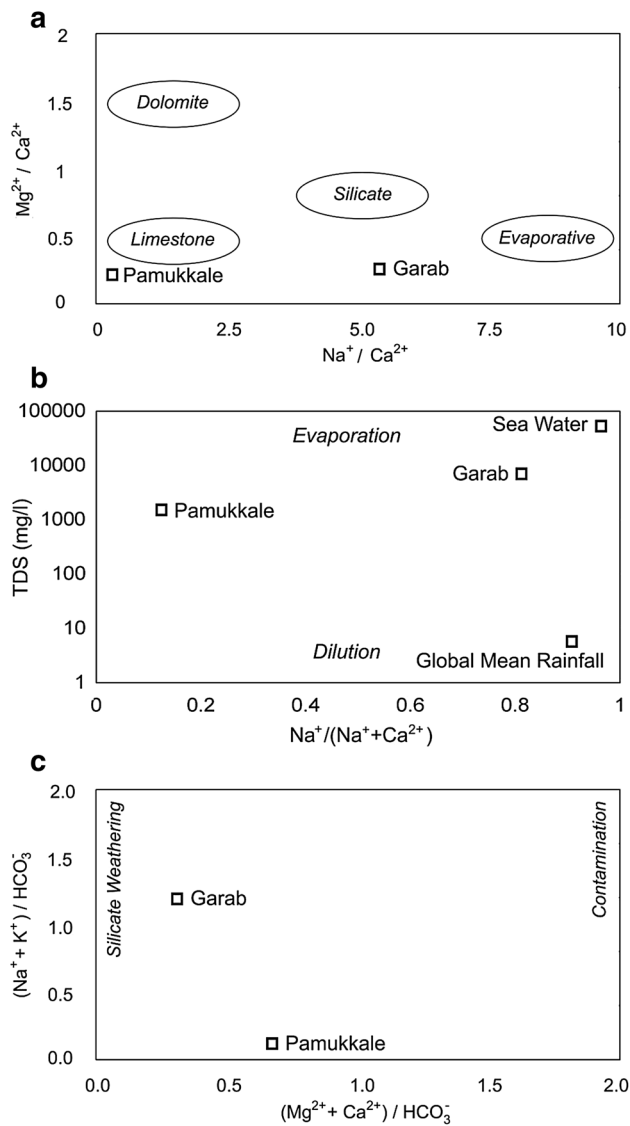


**Fig. 4** Geochemical plots of **a** Mg/Ca against Na/Ca, **b** TDS against Na/(Na+Ca), and **c** (Na+K)/HCO<sub>3</sub> against (Mg+Ca)/HCO<sub>3</sub> for water samples in both Garab and Pamukkale regions

## Discussion

### Controls on $\delta^{18}\text{O}$ and $\delta^2\text{H}$ compositions of Garab and Pamukkale spring water

Precipitation in both Garab (Mashhad meteoric water line: MMWL,  $\delta^2\text{H} = 7.2 \cdot \delta^{18}\text{O} + 11.2\text{‰}$ , Mohammadzadeh 2010) and Pamukkale (Western Anatolian meteoric water line: WAMWL,  $\delta^2\text{H} = 8 \cdot \delta^{18}\text{O} + 16\text{‰}$ , Şimşek 2003) areas are characterized by deuterium-excess (d-excess) values of 11.2‰ and 16‰, respectively (Fig. 6). Mentioned d-excess values of Garab and Pamukkale are greater than global meteoric water line (GMWL,  $\delta^2\text{H} = 8 \cdot \delta^{18}\text{O} + 10\text{‰}$ , Craig 1961), but smaller

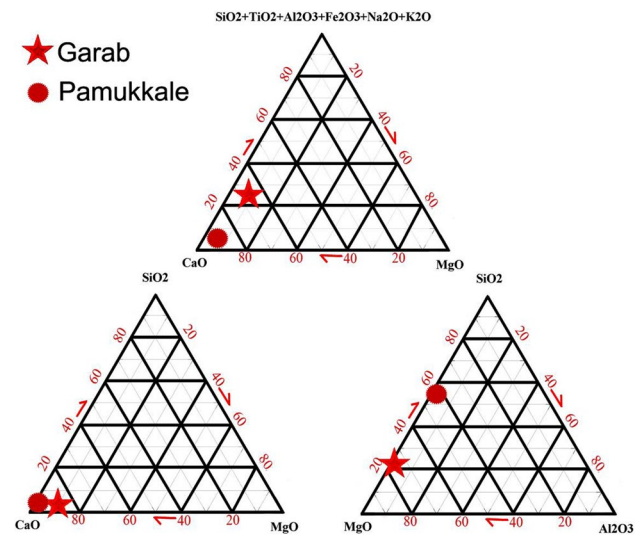


**Fig. 5** Plot of main ternary diagrams of CaO–MgO–SiO<sub>2</sub>, MgO–Al<sub>2</sub>O<sub>3</sub>–SiO<sub>2</sub>, and CaO–MgO–other compositions for water samples in both Garab and Pamukkale regions

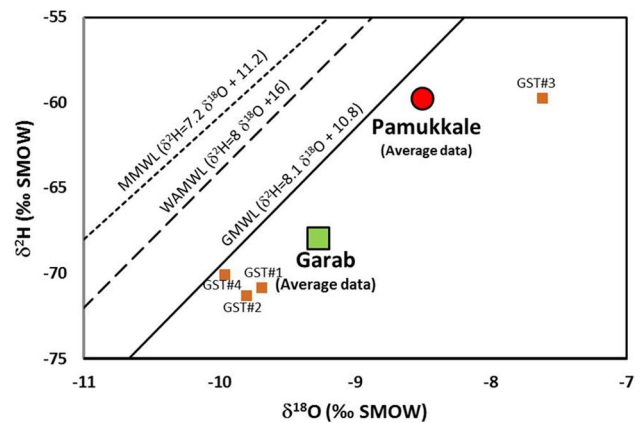


**Fig. 6** Stable isotope plot of  $\delta^{18}\text{O}$  against  $\delta^2\text{H}$  for water samples in both Garab and Pamukkale regions, GMWL: Global meteoric water line (Craig 1961), MMWL: Mashhad meteoric water line (Mohammadzadeh 2010), and WAMWL: Western Anatolian meteoric water line (Şimşek 2003)

than d-excess of Eastern Mediterranean meteoric water line (EMMWL,  $\delta^2\text{H} = 8 \cdot \delta^{18}\text{O} + 22\text{‰}$ , Gat and Carmi 1970), indicating the evaporation of seawater with hyper-arid atmospheric condition (Clark and Fritz 1997). Furthermore, the lower d-excess value of Garab compared to Pamukkale depends on the low quota of precipitation originating from the Mediterranean Sea in the Garab area (Mashhad) relative to the Pamukkale area (Anatolian Region). It is worth to be mentioned that the isotopic line of MMWL was developed by Mohammadzadeh (2010) and Mohammadzadeh and Heydarizad (2019) based on several rain samples taken from the Mashhad area, as shown in

Fig. 2c. Gat and Carmi (1970) and Şimşek (2003) have developed the isotopic lines of EMMWL and WAMWL based on the precipitation samples in the Buyuk Menderes basin and coastal stations of the eastern Mediterranean and Aegean Sea (Fig. 2c). In most stable isotope studies in Iran, the global meteoric water line (GMWL) and the Eastern Mediterranean meteoric water line (EMMWL) are used compared to local meteoric water lines (Heydarizad et al. 2019).

On  $\delta^{18}\text{O}$  vs.  $\delta^2\text{H}$  diagram (Fig. 6), all spring water from both Garab and Pamukkale regions were plotted below the GMWL. This finding indicates the similar origin of spring water in the Garab and Pamukkale regions, which are greatly affected by meteoric waters (Fig. 7). However, the deviation from local meteoric water lines and GMWL, is probably due to affected by oxygen isotope exchange with the deep host bedrock, because water–rock oxygen isotope exchange shifts the  $\delta^{18}\text{O}_{\text{water}}$  to a positive direction. The oxygen isotope exchange between water and rock supposedly takes place around and above 200 °C (Kele et al. 2011) while the temperatures of the Garab and Pamukkale spring are lower (24.3 and 36.7 °C, respectively). The most reasonable explanation is that hot water ascends along the tectonic lines and mixes to the shallow cool water resulting in 24.3 and 36.7 °C water at the Garab and Pamukkale springs, respectively. Among this process, especially in the Garab area, the water is enriched by the admixture of Na–Cl evaporitic lithology resulting in very high values of EC and TDS (~ 10,500  $\mu\text{s}/\text{cm}$  and ~ 6000, respectively). The slight rise in the average values of  $\delta^2\text{H}$  and  $\delta^{18}\text{O}$  in Pamukkale springs (about 9.3 and 0.6‰ VSMOW, Table 3 and Fig. 6), in compare with that of Garab spring water, probably is attributed to the effect of different deep of evaporation or can be related to precipitation of calcite and aragonite in different environments (Ozkul et al. 2002).

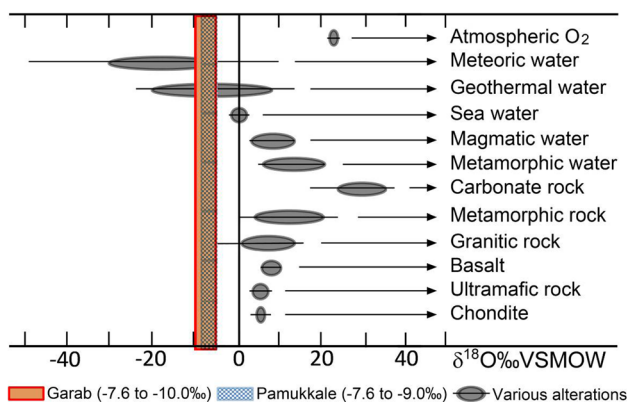


**Fig. 7** The range of  $\delta^{18}\text{O}$  compositions in Garab and Pamukkale waters, compared to the various alterations in the crustal rock or water types (Clark and Fritz 1997)

## Controls on $\delta^{13}\text{C}$ and $\delta^{18}\text{O}$ compositions of Garab and Pamukkale travertines

The preferential release of  $^{12}\text{CO}_2$  to the atmosphere, during rapid  $\text{CO}_2$  degassing from the water, results in a progressive increase of travertine  $\delta^{13}\text{C}$ . As the water flows upward toward the ground level, by changing the water conditions of temperature and pressure, it becomes oversaturated with respect to  $\text{CaCO}_3$ , and travertine is deposited. The stable  $^{13}\text{C}$  and  $^{18}\text{O}$  isotopic composition of travertines depends on deposition conditions and many other parameters such as the origin and  $\text{CO}_2$  escape; the primary/parent carbonate rock; microbiological activity; the parent karstic water reservoir of the travertine; local climate and T of water; and tectonism (Kele et al. 2011). To determine the  $\delta^{13}\text{C}$  of the  $\text{CO}_2$  released from the water during travertine deposition, we applied the Panichi and Tongiorgi (1976) equation ( $\delta^{13}\text{C}_{\text{CO}_2} = 1.2 * \delta^{13}\text{C}_{\text{travertine}} - 10.5$ ). Using the average measured  $\delta^{13}\text{C}_{\text{travertine}}$  values of Garab and Pamukkale (10.4 and 7.2‰ VPDB, respectively), this equation gives values of 1.5 and -1.8‰ VPDB for the  $\delta^{13}\text{C}$  of the  $\text{CO}_2$  released from the water during travertine deposition “original  $\text{CO}_2$ ” at Garab and Pamukkale areas, respectively (Table 3). These values are enriched than the  $\delta^{13}\text{C}$  of  $\text{CO}_2$  coming from magmatic sources, which has generally very low  $\delta^{13}\text{C}_{\text{CO}_2}$  values from -7 to -5‰ (Hoefs 1997). Consequently, the heat source cannot be related to volcanic activities, and it is most probably associated with the geothermal gradient with a deep circulation of groundwater through faults in both areas. In the Garab region, the presence of many fractures and joints are related to acting extensional fault systems of Shandiz-Sangbast (Zeraatkar and Rahimi 2012), which led to active tectonic and discharge of groundwater as hot springs (Goleij et al. 2018).

## Conclusion

The chemical property of the Garab spring water was identified as Na–Cl with very high values of EC and TDS as ~ 10,500  $\mu\text{s}/\text{cm}$  and ~ 6000 mg/l, respectively, which attributed to possible evaporating processes. The net concentration of  $\text{Ca}^{2+}$  and  $\text{Mg}^{2+}$  cations and  $\text{HCO}_3^-$  and  $\text{SO}_4^{2-}$  anions in both Garab and Pamukkale water samples represent similar ranges values, evidencing to carbonate origin in bedrocks. The more concentrations of  $\text{Na}^+$  and  $\text{K}^+$  cations and of  $\text{Cl}^-$  in Garab water are related to subsequent admixture processes, which is originate from dissolving overloaded impure dissolve materials during upwelling water toward the ground level. This can be confirmed by the much higher average value of EC and TDS in Garab water (10,428  $\mu\text{s}/\text{cm}$  and 5914 mg/l, respectively) than that of Pamukkale water (2400  $\mu\text{s}/\text{cm}$  and 1186 mg/l). The high TDS values of water

in Garab and Pamukkale regions are an indication of geothermal waters (Özler 2000) and it depends on the dissolution of carbonates from the calcareous rocks and leakage of the deep ground (Flores Márquez et al. 2006).

The d-excess values of precipitation in both Garab and Pamukkale areas (11.2‰ and 16.0‰, respectively) were greater than that of GMWL, but smaller than the d-excess of EMMWL, indicating the secondary evaporation process. The lower d-excess value of Garab compared to Pamukkale depends on the low quota of precipitation originating from the Mediterranean Sea in the Garab area (Mashhad) relative to the Pamukkale area (Anatolian Region). The  $\delta^{18}\text{O}$  and  $\delta^2\text{H}$  values of Garab spring water (−9.3 and −68.0‰ VSMOW, respectively) are almost similar to that of Pamukkale spring water (−8.7, −58.7‰).

The mean concentration values of free  $\text{CO}_2$  in both Garab and Pamukkale springs (316 mg/l and 673 mg/l, respectively) are more than 300 mg/l, indicating deep thermal waters (Dilsiz 2006). These travertine-depositing springs along structural zones suggest deeply source and endogenic  $\text{CO}_2$ -rich water cycle in the faults and fractures (Yoshimura et al. 2004). The average  $\delta^{13}\text{C}_{\text{DIC}}$  values of water samples in both Garab and Pamukkale regions (10.4‰ and 7.2‰ VPDB) indicate that the main source of the  $\text{CO}_2$  is a decomposition of marine carbonates with an origin in deep bedrock limestone. The evidence of carbonate rock was detected based on the plot of main ternary diagrams for both regions as well. Hence, the same carbonate bedrocks may influence the origin of both regions, where the calcium, bicarbonate, and sulfate concentrations originate from the dissolution of limestone and evaporate units. The more enriched  $\delta^{13}\text{C}_{\text{DIC}}$  value of Garab spring water than that of Pamukkale spring water indicates more contribution of carbonate dissolution in Garab spring water through the rock-water interactions process.

The continues  $\text{CO}_2$  degassing was observed in Garab spring water, which resulted in enriched  $\delta^{13}\text{C}$  and  $\delta^{18}\text{O}$  values of travertine rock samples (with an average value of 10.4 and −7.1‰ VPDB, respectively). The more enriched  $\delta^{13}\text{C}$  and  $\delta^{18}\text{O}$  values of Garab travertine than that of Pamukkale travertine (7.2 and −10.4‰ VPDB, respectively) are probably due to more  $\text{CO}_2$  degassing. The calculated  $\delta^{13}\text{C}$  values of the released  $\text{CO}_2$  from Garab and Pamukkale water during travertine deposition (1.5 and −1.8‰ VPDB, respectively) were enriched than the  $\delta^{13}\text{C}$  of  $\text{CO}_2$  originate from magmatic sources (with values ranging from −7 to −5‰ VPDB - Hoefs 1997). Consequently, the heat source cannot be related to volcanic activities, and it is most probably associated with the geothermal gradient with a deep circulation of groundwater through faults in both areas.

**Acknowledgements** We thank anonymous reviewers for technical suggestions on data interpretations.

## References

- Alçıçek H, Varol B, Özkul M (2007) Sedimentary facies, depositional environments and palaeogeographic evolution of the Neogene Denizli Basin, SW Anatolia. *Turk Sediment Geol* 202:596–637
- Altunel E (1994) Active tectonics and the evolution of Quaternary travertines at Pamukkale, Western Turkey. PhD thesis, University of Bristol, p 236
- Altunel E, Hancock PL (1993) Morphology and structural setting of Quaternary travertines at Pamukkale, Turkey. *Geol J* 28(3–4):335–346
- Anzalone E, Ferreri V, Sprovieri M, D'Argenio B (2007) Travertines as hydrologic archives: the case of the Pontecagnano deposits (southern Italy). *Adv Water Resour* 30(10):2159–2175
- Atabey E (2002) The formation of fissure ridge type laminated travertine-tufa deposits microscopical characteristics and diagenesis, Kirşehir, central Anatolia. *Bull Mineral Res Explor Inst Turkey* 123–124:59–70
- Bayari CS, Pekkan E, Ozyurt NN (2009) Obruks, as giant collapse dolines caused by hypogenic karstification in central Anatolia, Turkey: analysis of likely formation processes. *Hydrogeol J* 17(2):327–345
- Broggi A, Capezzuoli E (2009) Travertine deposition and faulting: the fault-related travertine fissure-ridge at Terme S. Giovanni, Rapolano Terme (Italy). *Int J Earth Sci* 98(4):931–947
- Broggi A, Capezzuoli E, Aqué R, Branca M, Voltaggio M (2010) Studying travertines for neotectonics investigations: middle-Late Pleistocene syn-tectonic travertine deposition at Serre di Rapolano (Northern Apennines, Italy). *Int J Earth Sci* 99(6):1383–1398
- Çakır Z (1999) Along-strike discontinuity of active normal faults and its influence on quaternary travertine deposition: examples from western Turkey. *Turk J Earth Sci* 8:67–80
- Chafetz HS, Guidry SA (2003) Deposition and diagenesis of mammoth hot springs travertine, yellowstone National Park, Wyoming, USA. *Can J Earth Sci* 40(11):1515–1529
- Clark ID, Fritz P (1997) Environmental isotopes in hydrogeology. Lewis Publishers, Boca Raton, FL, p 328
- Craig H (1961) Isotopic variation in meteoric waters. *Sci N.Y.* 133:1702–1703
- Crossey LJ, Fischer TP, Patchett PJ, Karlstrom KE, Hilton DR, Newell DL, Huntoon P, Reynolds AC, de Leeuw GAM (2006) Dissected hydrologic system at the Grand Canyon; interaction between deeply derived fluids and plateau aquifer waters in modern springs and travertine. *Geology* 34(1):25–28
- Di Benedetto F, Montegrossi G, Minissale A, Pardi LA, Romanelli M, Tassi F, Delgado Huertas A, Pampin EM, Vaselli O, Borini D (2011) Biotic and inorganic control on travertine deposition at Bullicame 3 spring (Viterbo, Italy): a multidisciplinary approach. *Geochim Cosmochim Acta* 75:4441–4455
- Dilsiz C (2006) Conceptual hydrodynamic model of the Pamukkale hydrothermal field, southwestern Turkey, based on hydrochemical and isotopic data. *Hydrogeol J* 14(4):562–572
- Domínguez-Villar D, Vázquez-Navarro JA, Krklec K (2017) The role of gypsum and/or dolomite dissolution in tufa precipitation: lessons from the hydrochemistry of a carbonate–sulphate karst system. *Earth Surf Proc Land* 42(2):245–258
- Ekmekeçi M, Günay G, Şimşek Ş (1995) Morphology of rim stone pools, Pamukkale, western Turkey. *Cave Karst Sci* 22:103–106
- Filiz S (1984) Investigation of the important geothermal areas by using C, H, O isotopes. In: Proceeding of the utilization of geothermal energy for electric power generation and space heating, Florence, Italy. Ref. No. EP/SEM.9/R.3
- Flores Márquez EL, Jiménez-Suárez G, Martínez-Serrano RG, Chávez RE, Silva-Pérez D (2006) Study of geothermal water

- intrusion due to groundwater exploitation in the Puebla Valley aquifer system, Mexico. *Hydrogeol J* 14(7):1216–1230
- Gat JR, Carmi I (1970) Evolution in the isotopic composition of atmospheric waters in the Mediterranean Sea area. *J Geophys Res* 75:3039–3048
- Goleij F, Mahboubi A, Khanehbad M, Moussavi-Harami R (2018) Sedimentology and hydro-geochemistry of Garab travertines in southeast of Mashhad, Iran. *Geopersia* 8(2):157–170
- Han GL, Liu CQ (2004) Water geochemistry controlled by carbonate dissolution: a study of the river waters draining karst-dominated terrain, Guizhou Province, China. *Chem Geol* 204:1–21
- Han GL, Tang Y, Xu ZF (2010) Fluvial geochemistry of rivers draining karst terrain in southwest China. *J Asian Earth Sci* 38:65–75
- Hancock PL, Altunel E (1997) Faulted archaeological relics at Hierapolis (Pamukkale), Turkey. *J Geodyn* 24:21–36
- Herhsey RL, Mizell SA, Earman S (2010) Chemical and physical characteristics of springs discharging from regional flow systems of the carbonate-rock province of the Great Basin, western United States. *Hydrogeol J* 18(4):1007–1026
- Heydarizad M, Raeisi E, Sorí R, Gimeno L (2019) Developing meteoric water lines for Iran based on air masses and moisture sources. *Water* 11(11):2359
- Hoefs J (1997) *Stable isotope geochemistry*. Springer, Berlin, p. p 201
- Karimpour MH, Stern CR, Farmer GL (2010) Zircon U-Pb geochronology, Sr-Nd isotope analyses, and petrogenetic study of the Dehnow diorite and Kuhsangi granodiorite (Paleo-Tethys), NE Iran. *J Asian Earth Sci* 37:384–393
- Kele S, Özkul M, Förizs I, Gökgöz A, Baykara MO, Alçiçek MC, Németh T (2011) Stable isotope geochemical study of Pamukkale travertines: new evidences of low-temperature non-equilibrium calcite water fractionation. *Sed Geol* 238:191–212
- Keshavarzi B, Moore F, Mosafieri M, Rahmani F (2011) The source of natural arsenic contamination in groundwater, west of Iran. *Water Qual Expos Health* 3:135–147
- Lang YC, Liu CQ, Zhao ZQ, Li SL, Han GL (2006) Geochemistry of surface and ground water in Guiyang, China: water/rock interaction and pollution in a karst hydrological system. *Appl Geochem* 21(6):887–903
- Ma R, Wang Y, Sun Z, Zheng C, Ma T, Prommer H (2011) Geochemical evolution of groundwater in carbonate aquifers in Taiyuan, northern China. *Appl Geochem* 26:884–897
- Mansouri Daneshvar MR (2015) Climatic impacts on hydrogeochemical characteristics of mineralized springs: a case study of the Garab travertine zone in the northeast of Iran. *Arab J Geosci* 8(7):4895–4906
- Mansouri Daneshvar MR, Pourali M (2015) Hydrogeochemical and geomorphological investigation of travertine deposition in the Garab Spring region, NE Iran. *Sustain Water Resour Manag* 1(3):253–262
- Minissale A, Kerrick DM, Magro G, Murrell MT, Paladini M, Rihs S, Sturchio NC, Tassi F, Vaselli O (2002) Geochemistry of Quaternary travertines in the region north of Rome (Italy): structural, hydrologic and paleoclimatic implications. *Earth Planet Sci Lett* 203(2):709–728
- Mohammadzadeh H (2009) The quality and isotope geochemistry of Garow saline water springs, Mashhad-Iran. *Proc Goldschmidt Conf* 73(13S):A891
- Mohammadzadeh H (2010) The meteoric relationship for  $^{18}\text{O}$  and  $^2\text{H}$  in precipitations and isotopic compositions of water resources in Mashhad area (NE Iran): the first Azad university international geology conference. Mashhad, pp 555–559
- Mohammadzadeh H, Clark ID (2011) Bioattenuation in groundwater impacted by landfill leachate traced with  $\delta^{13}\text{C}$ . *Ground Water* 49(6):880–890
- Mohammadzadeh H, Heydarizad M (2019)  $\delta^{18}\text{O}$  and  $\delta^2\text{H}$  characteristics of moisture sources and their role in surface water recharge in the north-east Iran. *Isot Environ Health Stud* 55(6):550–565
- Mohammadzadeh H, Kazemi M (2017) Geofluids assessment of the Ayub and Shafa hot springs in Kopet-Dagh zone (NE Iran): an isotopic geochemistry approach. *Geofluids*. <https://doi.org/10.1155/2017/6358680>
- Mohammadzadeh H, Clark ID, Marschner M, St-Jean G (2005) Compound specific isotopic analysis (CSIA) of landfill leachate DOC components. *Chem Geol* 218:3–13
- Özkul M, Varol B, Alçiçek MC (2002) Depositional environments and petrography of denizli travertines. *Miner Res Explor Bull* 125:13–29
- Özkul M, Gökgöz A, Horvatinčić N (2010) Depositional properties and geochemistry of Holocene perched springline tufa deposits and associated spring waters: a case study from the Denizli province, Western Turkey. In: Pedley HM (ed) *Tufas and speleothems: unravelling the microbial and physical controls*, the geological society, London. Special Publications vol 336, pp 245–262
- Özkul M, Kele S, Gökgöz A, Shen CC, Jones B, Baykara MO, Förizs I, Németh T, Chang YW, Alçiçek MC (2013) Comparison of the quaternary travertine sites in the Denizli extensional basin based on their depositional and geochemical data. *Sed Geol* 294:179–204
- Özler HM (2000) Water balance and water quality in the Çürüksu basin, western Turkey. *Hydrogeol J* 7(4):405–418
- Panichi C, Tongiorgi E (1976) Carbon isotopic composition of  $\text{CO}_2$  from springs, fumaroles, mofettes and travertines of central and southern Italy: a preliminary prospection method of geothermal areas. In: *Proceedings of the 2nd U.N. symposium on the development and use of geothermal energy*, San Francisco, 20–29 May 1975, pp 815–825
- Pazand K, Hezarkhani A, Ghanbari Y, Aghavali N (2012) Groundwater geochemistry in the Meshkinshahr basin of Ardabil province in Iran. *Environ Earth Sci* 65:871–879
- Pedley HM (2009) *Tufas and travertines of the Mediterranean region: a testing ground for freshwater carbonate concepts and developments*. *Sedimentology* 56:221–246
- Pentecost A (2005) *Travertine*. Springer Verlag, Berlin, p 445
- Petitta M, Primavera P, Tuccimei P, Aravena R (2011) Interaction between deep and shallow groundwater systems in areas affected by quaternary tectonics (Central Italy): a geochemical and isotope approach. *Environ Earth Sci* 63(1):11–30
- Piper AM (1944) A graphic procedure in the geochemical interpretation of water analysis. *Trans Am Geophys Union* 25(6):914–923
- Ryu JS, Lee KS, Chang HW (2007) Hydrogeochemical and isotopic investigations of the Han River Basin, South Korea. *J Hydrol* 345:50–60
- Şimşek Ş (2003) Hydrogeological and isotopic survey of geothermal fields in the Büyük Menderes graben, Turkey. *Geothermics* 32:669–678
- Şimşek S, Günay G, Elhatip H, Ekmeççi M (2000) Environmental protection of geothermal waters and travertines at Pamukkale, Turkey. *Geothermics* 29:557–572
- Uysal T, Feng Y, Zhao J, Altunel E, Weatherley D, Karabacak V, Cengiz O, Golding SD, Lawrence MG, Collerson KD (2007) U-series dating and geochemical tracing of late Quaternary travertines in co-seismic fissures. *Earth Planet Sci Lett* 257:450–462
- Von Eynatten H, Pawlowsky-Glahn V, Egozcue JJ (2002) Understanding perturbation on the simplex: a simple method to better visualize and interpret compositional data in ternary diagrams. *Math Geol* 34(3):249–257
- Yoshimura K, Liu Z, Cao J, Yuan D, Inokura Y, Noto M (2004) Deep source  $\text{CO}_2$  in natural waters and its role in extensive tufa deposition in the Huanglong Ravines, Sichuan, China. *Chem Geol* 205:141–153

- Zedef V, Russell MJ, Fallick AE, Hall AJ (2000) Genesis of vein stockwork and sedimentary magnesite and hydromagnesite deposits in the ultramafic terranes of southwestern Turkey: a stable isotope study. *Econ Geol* 95(2):429–445
- Zeraatkar K, Rahimi B (2012) Survey of Sangbast-Shandiz fault zone growth and geomorphological results. *J Geogr Reg Dev* 10(19):196–214 (**In Persian**)
- Zhang CL, Fouke BW, Bonheyo G, Peacock A, White DC, Huang Y, Romanek CS (2004) Lipid biomarkers and carbon-isotopes of

modern travertine deposits (Yellowstone National Park, USA): implications for biogeochemical dynamics in hot-spring systems. *Geochim Cosmochim Acta* 68:3157–3169

**Publisher's Note** Springer Nature remains neutral with regard to jurisdictional claims in published maps and institutional affiliations.